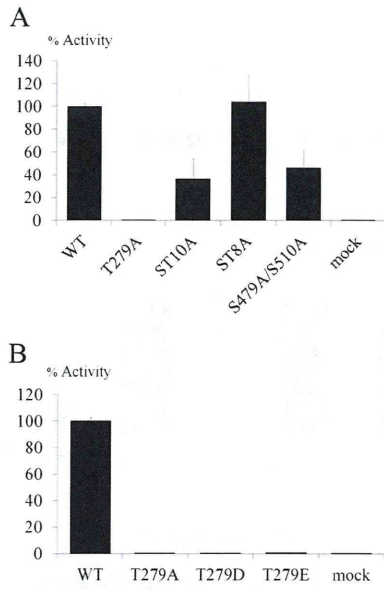

FIG 3 Functional analysis of minor phosphorylation sites. (A) Minigenome assay using the N protein mutants whose phosphorylation sites were substituted with alanine residue. 293 cells were transfected with minigenomic RNA and plasmids expressing the N, P, and L proteins. On the following day, the luciferase activity of the cell lysates was measured. (B) Minigenome assay using N-protein mutants with acidic residue substitutions at the T279 site.

The N protein possesses a nuclear localization signal and nuclear export signal for nucleocytoplasmic transport, and the N protein expressed alone in cultured cells localizes to the nucleus (35, 36). To investigate the significance of the T279 site, we examined the localization of the putative phosphorylation site mutants, including a series of T279 mutants, by indirect fluorescent-antibody (IFA) assay. The S479A S510A, ST8A, and ST10A N-protein mutants showed a nuclear localization identical to that of wt N protein, while T279 mutants showed a diffuse cytoplasmic distribution (Fig. 4A and B). Thus, T279 mutants showed abnormal properties by IFA assay. The P protein has been known to retain N protein in the cytoplasm and colocalizes with the N protein (36). In the presence of the P protein, the T279A mutant exhibited a dotted colocalization pattern with the P protein in the cytoplasm, similar to that seen for the wt N protein (Fig. 4C).

P protein is a major binding protein of the N protein and is required for viral transcription and replication (37, 38). The P protein functions as a carrier of the N protein to nascent replicating viral N-RNA complexes for efficient encapsidation (10), stabilizes NC by regulating the phosphorylation status of N protein (29), and prevents nonspecific binding of the N protein to host cellular RNA (10). To probe the mechanism of deactivation for the T279A mutant in a minigenome assay, we investigated the abilities of wt N protein and the T279A mutant N protein to bind to P protein by coimmunoprecipitation assay. Transiently coexpressed wt N or the T279A mutant N protein with P protein was labeled with ^{35}S and immunoprecipitated using anti-N polyclonal antibodies. There were no differences in coprecipitation of the P

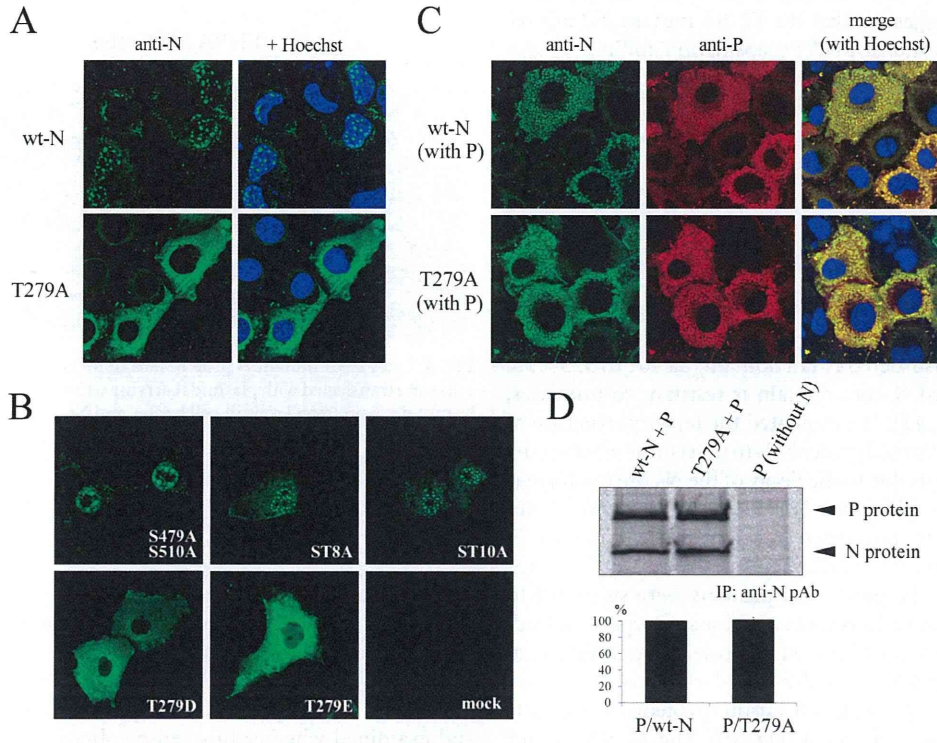

FIG 4 Localization and N-P binding ability of the T279A mutant. (A) T279 mutants showed a diffuse cytoplasmic distribution. Cos7 cells were transfected with a plasmid expressing wt N or T279A mutant N, and the localization of each protein was detected with anti-N polyclonal antibody. The localization of other N-protein mutants (B) and the distribution of wt N and T279A mutant N in the presence of the P protein (C) were evaluated. (D) wt N or T279A mutant N was transfected into Cos7 cells, along with the P protein. Proteins were labeled with ^{35}S and coprecipitated with anti-N polyclonal antibody (pAb). The bar graph shows the relative quantity of P protein coprecipitated with N protein (P protein/N protein). Error bars indicate standard deviations. IP, immunoprecipitation.

protein (Fig. 4D); this finding and the dotted colocalization with the P protein (Fig. 4C) suggest that the T279A mutant possesses a normal ability to bind to P protein, and therefore, the loss of activity of the T279A mutant in the minigenome assay was independent of N-P interactions.

T279 phosphorylation site of N protein is a prerequisite for NC formation. The region around T279 of the MV N protein is called CCR and has been reported to function as an N-N and N-RNA interaction domain to form NCs (34, 39, 40). Multiple-sequence alignment of CCRs among the *Paramyxoviridae* revealed that T279 is highly conserved (Fig. 2D). Therefore, we examined whether phosphorylation of the T279 site is required for NC formation. NC formation ability was tested by measuring and comparing the amount of NC-like particles in cells transfected with a plasmid expressing wt N protein or the T279A mutant N protein. The levels of expression of wt N protein and the T279A mutant N protein in Cos7 cells were similar, while the levels of purified NC-like particles from T279A mutant-transfected cell lysates were significantly reduced compared with those from wt N protein-transfected cell lysates (Fig. 5A). Thus, the alanine substitution at T279 caused a remarkable impairment of NC formation, and the T279 mutants showed a loss of activity in the minigenome assay.

Of note, the T279A mutants were detected in the NC fraction in the CsCl gradient centrifugation experiment (Fig. 5A), although the T279A mutant lost activity in the minigenome assay (Fig. 3A). To clarify that the N proteins acquired from the NC fraction formed correct NC structures, we subjected them to electron microscopy. The wt N protein showed a typical herringbone structure, while the T279A mutant from the NC fraction did not form a correct NC structure and aggregates of various sizes were detected (Fig. 5B), suggesting that the T279A mutant did not retain the self-assembly and/or RNA encapsidation ability.

Furthermore, we generated a plasmid containing the full genome with the T279A mutation in the N protein and attempted to rescue the T279A recombinant virus using a reverse genetics system that we had previously established (29, 41). However, we were unable to rescue the T279A mutant virus. This seems to be attributed to a loss of N-protein functions; the T279A mutant nucleoprotein could not correctly encapsidate the RNA (Fig. 5B) and did not support viral transcription and replication (Fig. 3A and B).

Phosphorylation of T279 is required for NC formation. N protein consists of a highly structured N core domain (aa 1 to 400) and an intrinsically disordered N tail domain (aa 401 to 525) (35, 38). A correctly folded N core domain is resistant to proteases, including trypsin (41, 42). We evaluated the tertiary structure of the T279A mutant by limited proteolysis to determine whether the loss of self-assembly was due to the decay of the N core conformation or the absence of phosphorylation. Plasmids for wt N and T279A mutant N were transfected into Cos7 cells, and each N protein was purified from the NC fraction obtained by CsCl gradient centrifugation. The purified N proteins were subjected to limited proteolysis with various concentrations of trypsin. Indeed, the 43.5-kDa core domain of the wt N protein was resistant to trypsin hydrolysis (Fig. 6A). Heat-denatured wt N protein showed a different degradation pattern, and various proteolytic products of less than 43.5 kDa were detected (Fig. 6B). The T279A mutant showed trypsin resistance, and its degradation pattern was identical to that of wt N protein (Fig. 6C). These results imply that the tertiary structure of the core domain of the T279A mutant retained its structural integrity. Thus, the alanine substitution of

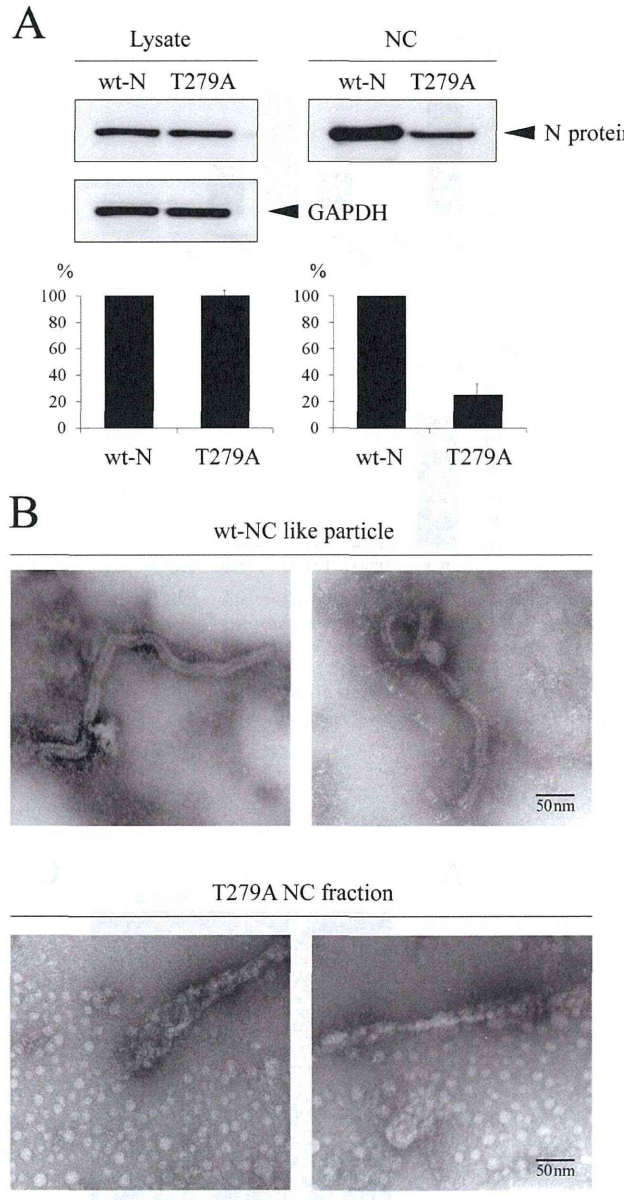

FIG 5 The T279A mutant N protein fails to form NC-like particles. (A) Cos7 cells were transfected with plasmids carrying wt N or T279A mutant N, and the N-protein expression levels in cell lysates and NC fractions obtained by CsCl density gradient centrifugation were determined and are shown here. Bar graphs indicate the relative levels of N-protein expression. Error bars indicate standard deviations. (B) Electron microscopy of wt N and T279A mutant N in the NC fraction obtained by CsCl density gradient centrifugation.

T279 did not cause denaturation of the tertiary structure of the N core domain, but the absence of T279 phosphorylation seemed to be critical for NC formation.

To investigate the significance of T279 phosphorylation on NC formation, we performed dephosphorylation of T279 with BAP and examined whether this caused abnormalities in NC formation. Previous reports demonstrated that deficient NC-like particles in Sendai virus could be discriminated by CsCl centrifugation (39, 41, 43). Using the same conditions, we examined whether this method was applicable to MV N protein. Lysates of wt N- and

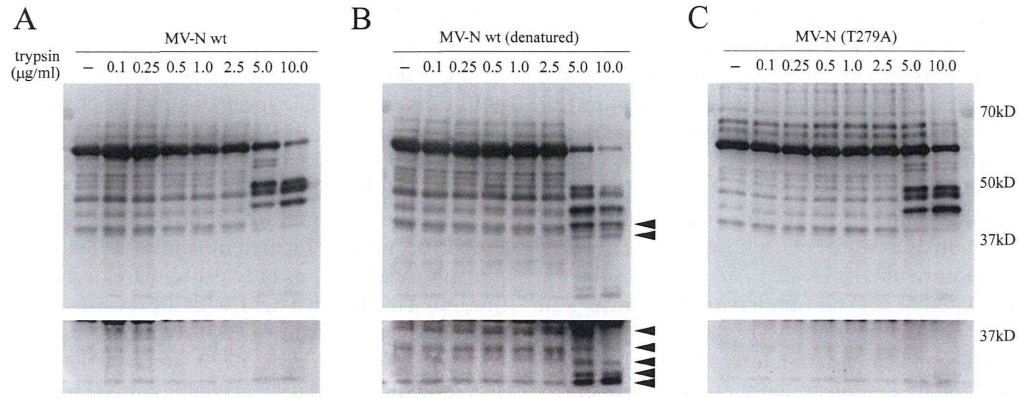

FIG 6 The T279A mutant N protein showed the same proteolytic pattern as wt N protein. The wt N, T279A mutant N, and heat-denatured wt N proteins were treated with various concentrations of trypsin. High-contrast images of the low-molecular-mass region (<37 kDa) are shown for low-density degradation products. Arrowheads, the various degradation products of the denatured N protein.

T279A mutant-transfected cells were subjected to CsCl gradient centrifugation to discriminate between normal and deficient NC-like particles. The gradients were divided into seven fractions, and the N protein in each fraction was detected by Western blotting. The NC-like particles of wt N were mainly detected in fractions 6 and 7 (Fig. 7A), while aggregates of the T279A mutant N protein were broadly detected from fractions 1 to 7 (Fig. 7B), indicating that the deficient NC-like particles formed aggregates of various sizes. Thus, normal NC-like particles could be discriminated from deficient aggregates. To demonstrate that T279 phosphorylation is important in NC formation, we then evaluated the influence of dephosphorylation of the ST10A mutant by examining whether the ST10A mutant could form normal NC-like particles in the presence or absence of BAP. The amino acids at all phosphorylation sites other than T279 were replaced by alanine residues in the ST10A mutant (Fig. 2A). Since there are no significant phosphorylation sites other than the 11 sites (Fig. 2B, E, and F), the influence of BAP treatment on the ST10A mutant was equivalent to that of T279 dephosphorylation. NC-like particles from the ST10A mutant were mainly detected in NC fractions 6 and 7, similar to the findings for intact NC-like particles, suggesting that the mutant ST10A formed normal NC-like particles (Fig. 7C). The ST10A mutant treated with BAP showed a wide distribution from fractions 2 to 7 (Fig. 7D), indicating that dephosphorylation of T279 caused a deficiency in NC formation. Furthermore, addition of a phosphatase inhibitor abrogated the NC deficiency caused by BAP treatment (Fig. 7E), indicating that it was not caused by binding of BAP to N protein but by dephosphorylation at T279. Taken together, these results suggest that phosphorylation at T279 is a prerequisite for NC formation.

DISCUSSION

We previously demonstrated that the major phosphorylation sites of N protein (S479 and S510) are involved in various stages of the viral life cycle (28, 29). Additionally, we found that a mutant with mutation of both major phosphorylation sites remained phosphorylated but to a lesser extent, suggesting that unidentified

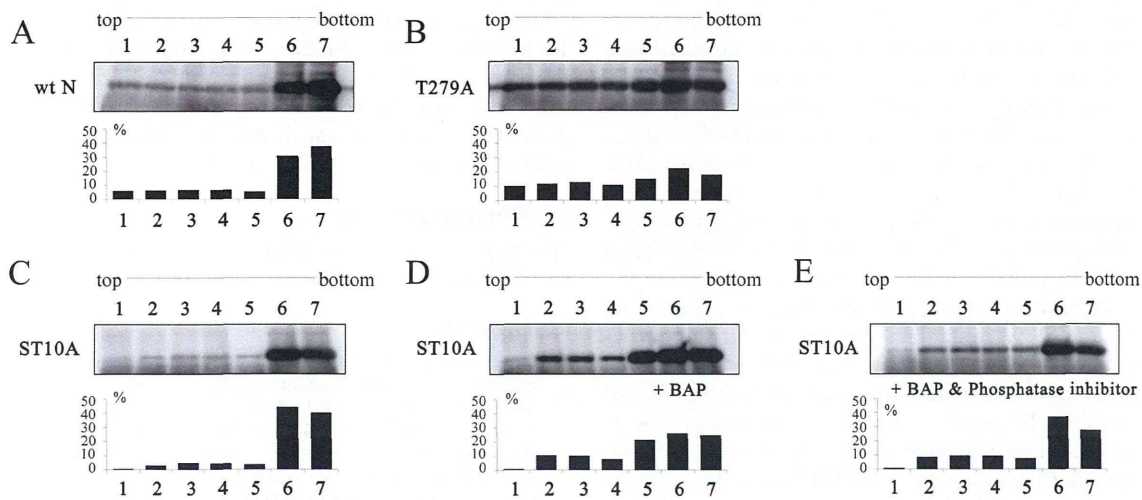

FIG 7 Dephosphorylation of T279 by BAP treatment impairs NC formation. NC-like particles of the wt N or N-protein mutants were separated by CsCl gradient centrifugation. Gradients were divided into 7 fractions, and the N protein in each fraction was detected. (A) wt N; (B) T279A mutant N; (C) ST10A mutant N; (D) ST10A mutant N with BAP treatment; (E) ST10A mutant N with BAP and phosphatase inhibitor treatment. Bar graphs show the percentage of N-protein content in each fraction per the total amount of N protein in the 7 fractions.

phosphorylation sites exist within the N protein. Here, we predicted the existence of nine putative minor phosphorylation sites of N protein by MS analysis. Moreover, we demonstrated that among the putative minor phosphorylation sites, a threonine residue at location 279 was notably phosphorylated and was a prerequisite for NC formation.

Since the late 1970s, it has been known that N protein undergoes phosphorylation at both serine and threonine residues and that the phosphorylation intensity of phosphoserine was stronger than that of phosphothreonine (44, 45). Additionally, in the 1990s, it was reported that the phosphorylation intensities of phosphoserine and phosphothreonine were 88% and 12%, respectively, of the total N phosphorylation intensity (46). In agreement with these reports, we demonstrated that the phosphorylation intensity of a mutant with mutations of both of the major phosphorylation sites (S479A and S510A) was 15.7% compared to that of wt N protein and the phosphorylation intensity of the T279 site was 14.3% of the total N phosphorylation intensity. This indicated that the intensity of major phosphorylation at serine residues was 84.3% and that almost all of the remaining 15.7% phosphorylation was due to phosphorylation of T279. Furthermore, specific phosphorylation was not detected in the ST11A mutant, suggesting the existence of no significant phosphorylation sites other than the 11 sites already identified. In addition, alanine substitution at putative minor phosphorylation sites other than T279 did not have an influence in a minigenome expression assay. Taken together, these data indicate that the functionally significant phosphorylation sites of N protein are limited to the two major phosphorylation sites (S479 and S510) and the minor T279 phosphorylation site.

It was reported that free N protein and NC-associated N protein showed different antigenicities toward antibodies, and this finding was explained to be the result of a conformational difference between the free N protein and NC-associated N protein (47–49). This suggests that conformational changes to N protein are required for NC formation. Furthermore, free N protein is phosphorylated only on serine residues, whereas the NC-associated N protein is phosphorylated on both serine and threonine residues (46), implying that threonine phosphorylation and subsequent conformational changes of N protein are prerequisites to NC formation. In agreement with these studies, we demonstrated by electron microscopy that the T279A mutant did not form NC-like particles. Additionally, our data also suggested that an absence of phosphorylation at the threonine residue resulted in a structural abnormality in the NC-like particle. Taken together, these data indicate that NC formation requires a conformational change of N protein that is switched by phosphorylation at T279. However, wt N protein and T279A mutant N protein harvested from NC fractions of CsCl density gradients did not show any difference in proteolytic peptide patterns after trypsin digestion, indicating that the T279A mutant retained a normal tertiary structure similar to that of the wt N protein. Thus, the conformational change required for NC formation was quite small and could not be discriminated by the use of trypsin digestion patterns. Indeed, trypsin digestion of free N protein and NC-associated N protein resulted in similar degradation patterns (46). Moreover, a mutant with double mutations of the MV N CCR domain whose SL (residues 228 and 229) amino acids were replaced by QD (NQD) did not show any differences from the wt in the results obtained by trypsin digestion analysis, immunoprecipitation, and circular dichroism (CD) spectroscopy, while the mutant did not form normal NC-like particles, as determined by electron microscopy (34). As the conformational change required for NC formation could not be detected by CD spectroscopy, the change was not accompanied by a change in secondary structure. Thus, in the NC formation step, very small conformational changes are required for correct encapsidation.

Since the CsCl gradient centrifugation assay suggested that the ST10A mutant formed normal NC-like particles, the major phosphorylation sites of N protein are dispensable for NC formation. This is consistent with a previous report demonstrating that the N tail region is not required for NC formation (43). Here, we identified the T279 site as a new phosphate group acceptor site that is indispensable for NC formation. However, the phosphorylation intensity of T279 was low, and this minor phosphorylation was only 14.3% of the total N phosphorylation. Moreover, replacement of T279 with acidic residues, such as aspartic acid and glutamic acid, also abrogated the phenotype of wt N protein in a minigenome assay and an IFA assay. Thus, the phosphorylation at T279 is not constitutive, and N protein is functionally inactive under circumstances where all N proteins are constantly phosphorylated at T279. Moreover, although the threonine residue of free N protein was not phosphorylated (46), 14.3% of the NC-associated N proteins were phosphorylated at T279. This indicates that one-seventh of the NC-associated N proteins are phosphorylated when N proteins incorporate into the nascent N-RNA complex. Whether N proteins were expressed by a plasmid or during viral replication (46), the phosphorylation rate of the threonine residue in NC was almost the same. Thus, T279 phosphorylation of the N protein is required for the maintenance of the herringbone-like structure of NC, and T279 is different from the major phosphorylation sites that take part in the functional regulation of viral gene expression (27–29). Electron microscopy demonstrated that NC has a helical structure with approximately 13 to 14 N proteins per turn (15, 50, 51). Therefore, N proteins may change their own conformation through the phosphorylation of T279 at a ratio of 1 per 7 to cancel the structural distortion of the NC.

In the present study, we demonstrated that phosphorylation at T279 is a prerequisite for NC formation. However, the relationship between T279 phosphorylation and conformational changes to NC-associated N proteins remains to be clarified. Further analysis of the conformational change in N protein might reveal the precise mechanism of NC formation.

ACKNOWLEDGMENTS

This study was supported by grants-in-aid from the Ministry of Education, Science, Sports, and Culture, Japan.

REFERENCES

1. **Centers for Disease Control and Prevention.** 2008. Progress in global measles control and mortality reduction, 2000-2007. MMWR Morb. Mortal. Wkly. Rep. **57**:1303–1306.
2. **Wolfson LJ, Strebel PM, Gacic-Dobo M, Hoekstra EJ, McFarland JW, Hersh BS.** 2007. Has the 2005 measles mortality reduction goal been achieved? A natural history modelling study. Lancet **369**:191–200. http://dx.doi.org/10.1016/S0140-6736(07)60107-X.
3. **Bryce J, Boschi-Pinto C, Shibuya K, Black RE.** 2005. WHO estimates of the causes of death in children. Lancet **365**:1147–1152. http://dx.doi.org/10.1016/S0140-6736(05)71877-8.
4. **Dowling PC, Blumberg BM, Menonna J, Adamus JE, Cook P, Crowley**

JC, Kolakofsky D, Cook SD. 1986. Transcriptional map of the measles virus genome. J. Gen. Virol. 67:1987–1992. http://dx.doi.org/10.1099/0022-1317-67-9-1987.
5. Cattaneo R, Kaelin K, Baczko K, Billeter MA. 1989. Measles virus editing provides an additional cysteine-rich protein. Cell 56:759–764. http://dx.doi.org/10.1016/0092-8674(89)90679-X.
6. Bellini WJ, Englund G, Rozenblatt S, Arnheiter H, Richardson CD. 1985. Measles virus P gene codes for two proteins. J. Virol. 53:908–919.
7. Gely S, Lowry DF, Bernard C, Jensen MR, Blackledge M, Costanzo S, Bourhis JM, Darbon H, Daughdrill G, Longhi S. 2010. Solution structure of the C-terminal X domain of the measles virus phosphoprotein and interaction with the intrinsically disordered C-terminal domain of the nucleoprotein. J. Mol. Recognit. 23:435–447. http://dx.doi.org/10.1002/jmr.1010.
8. Karlin D, Ferron F, Canard B, Longhi S. 2003. Structural disorder and modular organization in Paramyxovirinae N and P. J. Gen. Virol. 84:3239–3252. http://dx.doi.org/10.1099/vir.0.19451-0.
9. Cevik B, Holmes DE, Vrotsos E, Feller JA, Smallwood S, Moyer SA. 2004. The phosphoprotein (P) and L binding sites reside in the N-terminus of the L subunit of the measles virus RNA polymerase. Virology 327:297–306. http://dx.doi.org/10.1016/j.virol.2004.07.002.
10. Curran J. 1996. Reexamination of the Sendai virus P protein domains required for RNA synthesis: a possible supplemental role for the P protein. Virology 221:130–140. http://dx.doi.org/10.1006/viro.1996.0359.
11. Ramachandran A, Parisien JP, Horvath CM. 2008. STAT2 is a primary target for measles virus V protein-mediated alpha/beta interferon signaling inhibition. J. Virol. 82:8330–8338. http://dx.doi.org/10.1128/JVI.00831-08.
12. Shaffer JA, Bellini WJ, Rota PA. 2003. The C protein of measles virus inhibits the type I interferon response. Virology 315:389–397. http://dx.doi.org/10.1016/S0042-6822(03)00537-3.
13. Hashiguchi T, Maenaka K, Yanagi Y. 2011. Measles virus hemagglutinin: structural insights into cell entry and measles vaccine. Front. Microbiol. 2:247. http://dx.doi.org/10.3389/fmicb.2011.00247.
14. Ray J, Fujinami RS. 1987. Characterization of in vitro transcription and transcriptional products of measles virus. J. Virol. 61:3381–3387.
15. Bhella D, Ralph A, Yeo RP. 2004. Conformational flexibility in recombinant measles virus nucleocapsids visualised by cryo-negative stain electron microscopy and real-space helical reconstruction. J. Mol. Biol. 340:319–331. http://dx.doi.org/10.1016/j.jmb.2004.05.015.
16. Lund GA, Tyrrell DL, Bradley RD, Scraba DG. 1984. The molecular length of measles virus RNA and the structural organization of measles nucleocapsids. J. Gen. Virol. 65:1535–1542. http://dx.doi.org/10.1099/0022-1317-65-9-1535.
17. Calain P, Roux L. 1993. The rule of six, a basic feature for efficient replication of Sendai virus defective interfering RNA. J. Virol. 67:4822–4830.
18. Bitko V, Barik S. 2001. Phenotypic silencing of cytoplasmic genes using sequence-specific double-stranded short interfering RNA and its application in the reverse genetics of wild type negative-strand RNA viruses. BMC Microbiol. 1:34. http://dx.doi.org/10.1186/1471-2180-1-34.
19. Moyer SA, Baker SC, Horikami SM. 1990. Host cell proteins required for measles virus reproduction. J. Gen. Virol. 71:775–783. http://dx.doi.org/10.1099/0022-1317-71-4-775.
20. Rima BK, Duprex WP. 2009. The measles virus replication cycle. Curr. Top. Microbiol. Immunol. 329:77–102. http://dx.doi.org/10.1007/978-3-540-70523-9_5.
21. Plumet S, Duprex WP, Gerlier D. 2005. Dynamics of viral RNA synthesis during measles virus infection. J. Virol. 79:6900–6908. http://dx.doi.org/10.1128/JVI.79.11.6900-6908.2005.
22. Plumet S, Gerlier D. 2005. Optimized SYBR green real-time PCR assay to quantify the absolute copy number of measles virus RNAs using gene specific primers. J. Virol. Methods 128:79–87. http://dx.doi.org/10.1016/j.jviromet.2005.03.020.
23. Warnes A, Fooks AR, Dowsett AB, Wilkinson GW, Stephenson JR. 1995. Expression of the measles virus nucleoprotein gene in Escherichia coli and assembly of nucleocapsid-like structures. Gene 160:173–178. http://dx.doi.org/10.1016/0378-1119(95)00227-W.
24. Fooks AR, Stephenson JR, Warnes A, Dowsett AB, Rima BK, Wilkinson GW. 1993. Measles virus nucleocapsid protein expressed in insect cells assembles into nucleocapsid-like structures. J. Gen. Virol. 74:1439–1444. http://dx.doi.org/10.1099/0022-1317-74-7-1439.
25. Spehner D, Kirn A, Drillien R. 1991. Assembly of nucleocapsidlike structures in animal cells infected with a vaccinia virus recombinant encoding the measles virus nucleoprotein. J. Virol. 65:6296–6300.
26. Kolakofsky D, Le Mercier P, Iseni F, Garcin D. 2004. Viral DNA polymerase scanning and the gymnastics of Sendai virus RNA synthesis. Virology 318:463–473. http://dx.doi.org/10.1016/j.virol.2003.10.031.
27. Hagiwara K, Sato H, Inoue Y, Watanabe A, Yoneda M, Ikeda F, Fujita K, Fukuda H, Takamura C, Kozuka-Hata H, Oyama M, Sugano S, Ohmi S, Kai C. 2008. Phosphorylation of measles virus nucleoprotein upregulates the transcriptional activity of minigenomic RNA. Proteomics 8:1871–1879. http://dx.doi.org/10.1002/pmic.200701051.
28. Sugai A, Sato H, Yoneda M, Kai C. 2012. Phosphorylation of measles virus phosphoprotein at S86 and/or S151 downregulates viral transcriptional activity. FEBS Lett. 586:3900–3907. http://dx.doi.org/10.1016/j.febslet.2012.09.021.
29. Sugai A, Sato H, Yoneda M, Kai C. 2013. Phosphorylation of Measles virus nucleoprotein affects viral growth by changing gene expression and genomic RNA stability. J. Virol. 87:11684–11692. http://dx.doi.org/10.1128/JVI.01201-13.
30. Niwa H, Yamamura K, Miyazaki J. 1991. Efficient selection for high-expression transfectants with a novel eukaryotic vector. Gene 108:193–199. http://dx.doi.org/10.1016/0378-1119(91)90434-D.
31. Kobune F, Takahashi H, Terao K, Ohkawa T, Ami Y, Suzaki Y, Nagata N, Sakata H, Yamanouchi K, Kai C. 1996. Nonhuman primate models of measles. Lab. Anim. Sci. 46:315–320.
32. Huang M, Sato H, Hagiwara K, Watanabe A, Sugai A, Ikeda F, Kozuka-Hata H, Oyama M, Yoneda M, Kai C. 2011. Determination of a phosphorylation site in Nipah virus nucleoprotein and its involvement in virus transcription. J. Gen. Virol. 92:2133–2141. http://dx.doi.org/10.1099/vir.0.032342-0.
33. Liston P, Batal R, DiFlumeri C, Briedis DJ. 1997. Protein interaction domains of the measles virus nucleocapsid protein (NP). Arch. Virol. 142:305–321. http://dx.doi.org/10.1007/s007050050078.
34. Karlin D, Longhi S, Canard B. 2002. Substitution of two residues in the measles virus nucleoprotein results in an impaired self-association. Virology 302:420–432. http://dx.doi.org/10.1006/viro.2002.1634.
35. Sato H, Masuda M, Miura R, Yoneda M, Kai C. 2006. Morbillivirus nucleoprotein possesses a novel nuclear localization signal and a CRM1-independent nuclear export signal. Virology 352:121–130. http://dx.doi.org/10.1016/j.virol.2006.04.013.
36. Huber M, Cattaneo R, Spielhofer P, Orvell C, Norrby E, Messerli M, Perriard JC, Billeter MA. 1991. Measles virus phosphoprotein retains the nucleocapsid protein in the cytoplasm. Virology 185:299–308. http://dx.doi.org/10.1016/0042-6822(91)90777-9.
37. Bernard C, Gely S, Bourhis JM, Morelli X, Longhi S, Darbon H. 2009. Interaction between the C-terminal domains of N and P proteins of measles virus investigated by NMR. FEBS Lett. 583:1084–1089. http://dx.doi.org/10.1016/j.febslet.2009.03.004.
38. Bourhis JM, Receveur-Bréchot V, Oglesbee M, Zhang X, Buccellato M, Darbon H, Canard B, Finet S, Longhi S. 2005. The intrinsically disordered C-terminal domain of the measles virus nucleoprotein interacts with the C-terminal domain of the phosphoprotein via two distinct sites and remains predominantly unfolded. Protein Sci. 14:1975–1992. http://dx.doi.org/10.1110/ps.051411805.
39. Myers TM, Smallwood S, Moyer SA. 1999. Identification of nucleocapsid protein residues required for Sendai virus nucleocapsid formation and genome replication. J. Gen. Virol. 80:1383–1391.
40. Terao-Muto Y, Yoneda M, Seki T, Watanabe A, Tsukiyama-Kohara K, Fujita K, Kai C. 2008. Heparin-like glycosaminoglycans prevent the infection of measles virus in SLAM-negative cell lines. Antiviral Res. 80:370–376. http://dx.doi.org/10.1016/j.antiviral.2008.08.006.
41. Myers TM, Pieters A, Moyer SA. 1997. A highly conserved region of the Sendai virus nucleocapsid protein contributes to the NP-NP binding domain. Virology 229:322–335. http://dx.doi.org/10.1006/viro.1996.8429.
42. Heggeness MH, Scheid A, Choppin PW. 1981. The relationship of conformational changes in the Sendai virus nucleocapsid to proteolytic cleavage of the NP polypeptide. Virology 114:555–562. http://dx.doi.org/10.1016/0042-6822(81)90235-X.
43. Buchholz CJ, Spehner D, Drillien R, Neubert WJ, Homann HE. 1993. The conserved N-terminal region of Sendai virus nucleocapsid protein NP is required for nucleocapsid assembly. J. Virol. 67:5803–5812.

44. **Robbins SJ, Fenimore JA, Bussell RH.** 1980. Structural phosphoproteins associated with measles virus nucleocapsids from persistently infected cells. J. Gen. Virol. **48**:445–449. http://dx.doi.org/10.1099/0022-1317-48-2-445.
45. **Robbins SJ, Bussell RH.** 1979. Structural phosphoproteins associated with purified measles virions and cytoplasmic nucleocapsids. Intervirology **12**:96–102. http://dx.doi.org/10.1159/000149074.
46. **Gombart AF, Hirano A, Wong TC.** 1995. Nucleoprotein phosphorylated on both serine and threonine is preferentially assembled into the nucleocapsids of measles virus. Virus Res. **37**:63–73. http://dx.doi.org/10.1016/0168-1702(95)00020-Q.
47. **Kawai A, Toriumi H, Tochikura TS, Takahashi T, Honda Y, Morimoto K.** 1999. Nucleocapsid formation and/or subsequent conformational change of rabies virus nucleoprotein (N) is a prerequisite step for acquiring the phosphatase-sensitive epitope of monoclonal antibody 5-2-26. Virology **263**:395–407. http://dx.doi.org/10.1006/viro.1999.9962.
48. **Gombart AF, Hirano A, Wong TC.** 1993. Conformational maturation of measles virus nucleocapsid protein. J. Virol. **67**:4133–4141.
49. **Hirano A, Wang AH, Gombart AF, Wong TC.** 1992. The matrix proteins of neurovirulent subacute sclerosing panencephalitis virus and its acute measles virus progenitor are functionally different. Proc. Natl. Acad. Sci. U. S. A. **89**:8745–8749. http://dx.doi.org/10.1073/pnas.89.18.8745.
50. **Kolakofsky D, Roux L, Garcin D, Ruigrok RW.** 2005. Paramyxovirus mRNA editing, the "rule of six" and error catastrophe: a hypothesis. J. Gen. Virol. **86**:1869–1877. http://dx.doi.org/10.1099/vir.0.80986-0.
51. **Bhella D, Ralph A, Murphy LB, Yeo RP.** 2002. Significant differences in nucleocapsid morphology within the Paramyxoviridae. J. Gen. Virol. **83**:1831–1839.

JVI
Journals.ASM.org

Phosphorylation of Measles Virus Nucleoprotein Affects Viral Growth by Changing Gene Expression and Genomic RNA Stability

Akihiro Sugai,[a] Hiroki Sato,[b] Misako Yoneda,[b] Chieko Kai[a,b]

International Research Center for Infectious Diseases[a] and Laboratory Animal Research Center,[b] The Institute of Medical Science, The University of Tokyo, Tokyo, Japan

The measles virus (MV) nucleoprotein associates with the viral RNA genome to form the N-RNA complex, providing a template for viral RNA synthesis. In our previous study, major phosphorylation sites of the nucleoprotein were identified as S479 and S510. However, the functions of these phosphorylation sites have not been clarified. In this study, we rescued recombinant MVs (rMVs) whose phosphorylation sites in the nucleoprotein were substituted (rMV-S479A, rMV-S510A, and rMV-S479A/S510A) by reverse genetics and used them in subsequent analyses. In a one-step growth experiment, rMVs showed rapid growth kinetics compared with wild-type MV, although the peak titer of the wild-type MV was the same as or slightly higher than those of the rMVs. Time course analysis of nucleoprotein accumulation also revealed that viral gene expression of rMV was enhanced during the early phase of infection. These findings suggest that nucleoprotein phosphorylation has an important role in controlling viral growth rate through the regulation of viral gene expression. Conversely, multistep growth curves revealed that nucleoprotein-phosphorylation intensity inversely correlated with viral titer at the plateau phase. Additionally, the phosphorylation intensity of the wild-type nucleoprotein in infected cells was significantly reduced through nucleoprotein-phosphoprotein binding. Excessive nucleoprotein-phosphorylation resulted in lower stability against RNase and faster turnover of viral genomic RNA. These results suggest that nucleoprotein-phosphorylation is also involved in viral genomic RNA stability.

Measles virus (MV), a *Morbillivirus* within the *Paramyxoviridae* family, is a highly contagious human pathogen, especially in developing countries (1). MV is a negative-stranded RNA virus with a genome that comprises six structural genes encoding the nucleoprotein (N), phosphoprotein (P), matrix protein (M), fusion protein (F), hemagglutinin protein (H), and large protein (L). The N protein is the most abundant viral protein in infected cells (2). The L protein is an RNA-dependent RNA polymerase, and the P protein is a multifunctional protein that mainly functions as a cofactor of the L protein (3, 4). The M protein assists with virus assembly (5, 6), and the F and H proteins mediate membrane fusion and binding to host cellular receptors, respectively (7).

The N protein is most associated with encapsidation of viral genomic and antigenomic RNA (8), with N proteins tightly associating with the viral genome to form an N-RNA complex, which in turn forms a herringbone structure (8, 9). N proteins typically associate with every six nucleotide bases to completely cover the 15,894-nucleotide viral RNA genome (10). This tight association of N with the genome makes it resistant to RNases and small interfering RNAs (siRNAs) (11, 12). Viral transcription and replication are conducted on the N-RNA complex in association with the P and L proteins. During replication, nascent growing viral RNA molecules are immediately encapsidated by the N protein (8, 13, 14). Thus, the uncapped full-length viral antigenome is produced and serves as a template for genome replication (15).

It has been reported that the MV N protein undergoes phosphorylation, and in a previous report we identified the major phosphorylation sites of the MV N protein as S479 and S510 (16). We also showed that the major phosphorylation sites of the N protein are indirectly involved in the regulation of viral transcription by changing the phosphorylation status of the P protein (17). In the present study, we rescued recombinant MV (rMV) HL strains (18) of these N-phosphorylation sites (S479A, S510A, and S479A/S510A) using a reverse genetics system that we had previously established (19) and investigated their influence on virus growth.

MATERIALS AND METHODS

Cells, viruses, plasmids, and antibodies. B95a cells (Epstein-Barr virus-transformed marmoset B-lymphoblastoid cells) (20, 21) were propagated in RPMI 1640 medium (Sigma) supplemented with 5% fetal bovine serum (JRH Bioscience), 2 mM L-glutamine, 100 U/ml penicillin, and 0.1 mg/ml streptomycin at 37°C/5% CO_2. HEK293 and 293SLAM cells (HEK293 cells stably expressing the signaling lymphocyte activation molecule [SLAM], which is a cellular receptor for MV) (22, 23) were maintained in Dulbecco's modified Eagle's medium (Sigma) with the same supplements as described above. The virulent MV-HL strain (18) and its recombinant viruses were propagated and titrated in B95a cells. The generation of the pCAGGS mammalian expression vectors (24) containing wild-type N (wt-N), N mutants (S479A, S510A, S479A/S510A, and 74–77A), and P and M genes from the MV-HL strain along with anti-N, -P, and -M polyclonal antibodies and anti-N protein monoclonal antibody 8G was performed as previously described (16, 25).

Rescue of rMVs. Amplification of the MV N mutant genes (S479A, S510A, and S479A/S510A) was conducted by PCR using TaKaRa LA *Taq* (TaKaRa Bio) and primers F (5′-CGG CGG CCG CTT CAC GAT GGC CAC ACT TTT GAG G-3′; NotI site underlined) and R (5′-CAG GCC GGC CCT AGT CTA GAA GAT CTC T-3′; FseI site underlined). The amplicons were cloned into pCR2.1 TOPO (TOPO TA cloning kit; Invitrogen) vector according to the manufacturer's instructions. The resulting plasmids were transformed into *Escherichia coli* DH5α cells, grown, and then digested with NotI and FseI (TaKaRa Bio) and fragments inserted between the NotI and FseI sites of the MeV-HL full genomic plasmid (7+)

Received 2 May 2013 Accepted 17 August 2013
Published ahead of print 21 August 2013
Address correspondence to Chieko Kai, ckai@ims.u-tokyo.ac.jp.

doi:10.1128/JVI.01201-13

(19) to replace the wt-N gene. Rescue of the recombinant viruses was conducted as previously reported (19). Briefly, vaccinia virus-infected HEK293 cells were transfected with N, P, and L protein expression plasmids and with the MV full-genome plasmid whose N protein was mutated at phosphorylation sites (pMDBI-wt, S479A, S510A, and S479A/S510A). B95a cells were added onto transfected HEK293 cells 2 days after transfection. When an adequate cytopathic effect was observed, infected cells were subjected to three freeze-thaw cycles followed by sonication. After removal of cellular debris, recombinant viruses in the supernatant were concentrated by centrifugation (25,000 rpm, 2 h, 4°C) in an Sw28 rotor (Beckman), and the viral pellet was dissolved in an appropriate volume of phosphate-buffered saline (PBS). Viral titers were expressed as the 50% tissue culture infectious dose per milliliter ($TCID_{50}$/ml) and were measured in B95a cells. Reverse transcription (RT) and direct sequencing using viral RNA extracted from infected cells of each recombinant virus were conducted to ensure that substitutions in the phosphorylation sites were contained in the N protein gene of the recombinant viruses.

Immunoprecipitation assay. HEK293 cells were transfected with plasmids expressing wt-N and N mutants (S479A, S510A, S479A/S510A, and 74–77A), with or without the P plasmid. At 24 h posttransfection, 0.38 mCi/ml ^{32}P (Phosphorus-32 Radionuclide; PerkinElmer) or 0.06 mCi/ml ^{35}S (EasyTag Express Protein Labeling Mix; PerkinElmer) was added to the medium, and the reaction mixture was incubated at 37°C for 24 h. Cells were harvested and lysed using lysis buffer (0.5 mM EDTA–0.5% Triton X-100–PBS) supplemented with Protease Inhibitor Cocktail (BD Biosciences) and PhosSTOP Phosphatase Inhibitor Cocktail (Roche Applied Science) for 1 h at 4°C. Cell debris was removed from the lysate by centrifugation. Lysates were incubated with protein A Sepharose CL-4B (Amersham Biosciences) and anti-N or -P polyclonal antibodies for 16 h at 4°C. Beads were washed five times with PBS and suspended in 2× Laemmli's sodium dodecyl sulfate (SDS) sample buffer. Proteins were separated by SDS-polyacrylamide gel electrophoresis (PAGE), and radioactivity was detected using an Imaging Plate and FLA-5100 phosphorimager (Fujifilm). Experiments were independently performed two or three times. The principle of the Imaging Plate method is as follows: the photostimulable phosphor on the Imaging Plate stores radiation energy by the electrical change from the ground state to the excited state. The stored excitation energy is converted to chemiluminescence by laser scanning of the phosphorimager, and the data are saved in a digital format. This detection system enables quantitative analysis of phosphorylation within a linear range.

293SLAM cells (5×10^5) were infected with wild-type or rMV-HL viruses. We then added ^{32}P (0.38 mCi/ml) and ^{35}S (0.06 mCi/ml) to the medium just after infection, and viruses were labeled until infected cells were harvested. At each time point from 16 h postinfection (hpi) to 6 days postinfection (dpi), cells were harvested and lysed. Following immunoprecipitation, SDS-PAGE and imaging were carried out as described above.

One-step and multistep growth kinetics. We infected 293SLAM cells with wt or recombinant viruses at a multiplicity of infection (MOI) of 1.0 or 0.001, in duplicate. The infected cells and supernatant were harvested at 4, 8, 12, 16, 20, and 24 hpi (MOI = 1.0) and at 12, 24, 48, 72, 96, 120, and 144 hpi (MOI = 0.001), respectively. After three cycles of freeze-thawing and sonication of infected cells, lysates were centrifuged to remove cellular debris, and the supernatant was collected. The titer ($TCID_{50}$/ml) of each sample was measured using B95a cells.

Western blot analysis. The 293SLAM cells infected with MVs were washed in PBS and lysed in buffer (0.5 mM EDTA–0.5% Triton X-100–PBS) containing Protease Inhibitor Cocktail at 8, 16, 20, and 24 hpi (MOI = 1.0) and at 2, 3, 4, 5, and 6 dpi (MOI = 0.001). The HEK293 cells transfected with expression plasmids using FuGENE 6 Transfection Reagent (Roche Applied Science) were lysed at 48 h posttransfection. Each lysate was separated by 8% or 10% SDS-PAGE and transferred onto an Immobilon-P Transfer Membrane (Millipore). Membranes were blocked with BlockACE (DS Pharma Biomedical) and then incubated with a primary antibody for 1 h at 37°C. The membrane was washed five times with PBS containing 0.05% Tween 20 and incubated with a polyclonal rabbit anti-mouse IgG conjugated to horseradish peroxidase (Dako Cytomation) (1:2,000 dilution) for 1 h at 37°C. Immunoreactive bands were visualized using ECL Western blotting detection reagents (GE Healthcare). Detection and scanning of chemiluminescence were performed with a luminescent image analyzer (LAS-1000UV mini system; Fujifilm).

Measurement of IFN-β and RANTES levels. The 293SLAM cells were infected with wt-MV or rMVs at an MOI of 1.0. Total RNA was extracted with Isogen (Nippon Gene) at 24 hpi, and RT was conducted with a 1:1 mixture of oligo(dT) primers and random hexamers and with PrimeScript RTase (TaKaRa) according to the manufacturer's instruction. Quantitative PCR (qPCR) assays were conducted using beta interferon (IFN-β)-specific (5′-CAG CAG TTC CAG AAG GAG GA-3′ and 5′-AGC CAG GAG GTT CTC AAC AA-3′) and RANTES-specific (5′-TCA TCC TCA TTG CTA CTG CC-3′ and 5′-GGT GAC AAA GAC GAC TGC TG-3′) primers and SYBR Premix *Ex Taq* (TaKaRa). GAPDH (glyceraldehyde-3-phosphate dehydrogenase) was used as an internal control, and expression levels were determined with specific primers (5′-AAC ATC ATC CCT GCC TCT ACT G-3′ and 5′-GCT TCA CCA CCT TCT TGA TGT C-3′). All qPCR assays were conducted on a Rotor-Gene Q cycler (Qiagen).

Indirect immunofluorescence assays. The HEK293 cells were transfected with expression vectors for wt-N, N protein mutants (S479A, S510A, S479A/S510A, and 74–77A), and the P protein using FuGENE 6 Transfection Reagent, according to the manufacturer's instructions. At 24 h posttransfection, cells were fixed with 3% paraformaldehyde–PBS and permeabilized with 0.5% Triton X-100–PBS. Cells were incubated with an anti-N protein polyclonal antibody followed by incubation with Alexa Fluor 488-conjugated goat anti-rabbit IgG (Invitrogen) (1:2,000) supplemented with Hoechst 33342 (Cambrex Bio Science). A confocal laser-scanning microscope (Fluoview FV1000-D system; Olympus) was used to visualize the fluorescence.

Complex formation assay. We transfected HEK293 cells with plasmids expressing wt-N and N mutants and with P or M proteins. Cells were lysed at 48 h posttransfection, and the cell lysates of N, P, and M protein-transfected cells were mixed and incubated for 1 h at 4°C. N, P, and M protein complexes were immunoprecipitated with 8G anti-N protein monoclonal antibody. Coprecipitated N, P, and M proteins were separated by SDS-PAGE and detected by immunoblotting using anti-N, -P, and -M protein polyclonal antibodies.

Pulse-chase assay. The 293SLAM cells infected with wt-MV or N protein rMVs (S479A, S510A, and S479A/S510A) at an MOI of 0.01 were labeled with [5,6-^{3}H]uridine (20 μCi/ml, PerkinElmer) for 18 h between 6 and 24 hpi. The culture medium was replaced with medium containing excess UTP (Roche) (200 nM/ml) and ribavirin (250 μM) at 1 dpi to stop the incorporation of [5,6-^{3}H]uridine. Infected cells were harvested and lysed at 0, 6, 24, and 48 h after the medium change. The released viruses were precipitated by centrifugation and lysed with infected cells. The nucleocapsid proteins in the lysate were separated by 25% to 40% sucrose gradient density centrifugation at 55,000 rpm for 1 h (Sw55Ti Rotor; Beckman). A Tri-Carb 2100TR Liquid Scintillation Analyzer (PerkinElmer) was used to measure radioactivity.

RNase protection assay. We infected 293SLAM cells with wt-MV or rMVs (S479A, S510A, and S479A/S510A) at an MOI of 0.001. Infected cells were divided into two equal portions after 5 days of incubation. One portion was lysed with micrococcal nuclease (MNase) buffer (10 mM Tris-HCl [pH 7.5], 10 mM NaCl, 5 mM $MgCl_2$, 2 mM $CaCl_2$, 1% Triton X-100, 0.5% sodium deoxycholate, BaculoGold Protease Inhibitor Cocktail [BD Biosciences], and 100 U/ml DNase) and treated with TRIzol LS (Invitrogen) to extract RNA. The other portion was lysed with MNase buffer supplemented with 100 U/ml MNase for 1 h at 37°C followed by RNA extraction with TRIzol LS. From the extracted RNAs, the viral genomic RNA was quantified by RT-PCR to calculate the protection rate from MNase. The RT reaction was conducted with MV genome RT

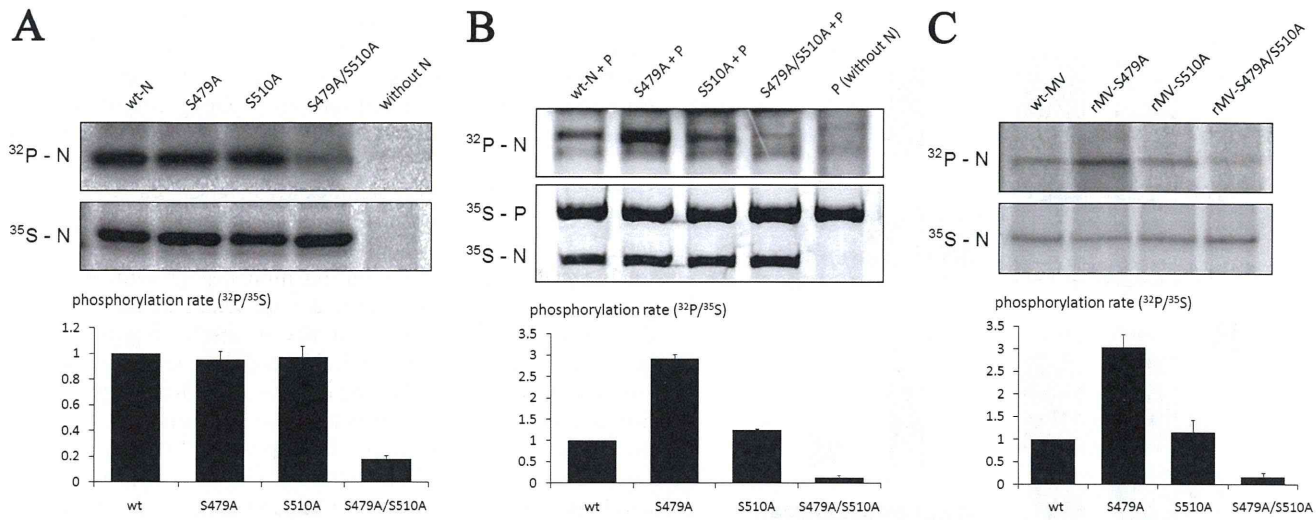

FIG 1 Phosphorylation status of wt-N protein and phosphorylation mutants (S479A, S510A, and S479A/S510A) under various conditions. (A) HEK293 cells were transfected with pCAGGS expression vectors encoding wt or mutant N proteins. N proteins expressed alone in HEK293 cells were labeled with ^{32}P or ^{35}S and precipitated with an anti-N polyclonal antibody. (B) N proteins were transiently expressed with the P protein in HEK293 cells, labeled with ^{32}P or ^{35}S, and coimmunoprecipitated with the P protein using an anti-P polyclonal antibody and quantified. (C) 293SLAM cells were infected with wt or rMVs (rMV-S479A, rMV-S510A, and rMV-S479A/S510A) at an MOI of 0.001 and labeled with ^{32}P or ^{35}S. The bar graphs below each image represent relative phosphorylation levels (^{32}P-N/^{35}S-N) for each N protein.

primer (5′-GGC CGT CAT GGT GGC GAA TCC TAC CTC GAC CTG TTG TTG AAT GAA GAG TTA GAA GAG TTC AC-3′) and PrimeScript RTase (TaKaRa), according to the manufacturer's instructions. Subsequently, qPCR assays were conducted with forward (5′-GGC CGT CAT GGT GGC GAA T-3′) and reverse (5′-TGT TCC ACG AAG ATC CT-3′) primers and SYBR Premix *Ex Taq* (TaKaRa) on a Rotor-Gene Q cycler. Genomic RNA quantities from MNase-treated and untreated samples were compared to calculate the protection rate.

RESULTS

N-P protein interaction alters the phosphorylation pattern of the N protein. In our previous report, it was suggested that the interaction between the N and P proteins affects the N protein phosphorylation status (17). We first compared the phosphorylation statuses of wt-N and its phosphorylation site mutants (S479A, S510A, and S479A/S510A) in the presence or absence of the P protein. ^{32}P- or ^{35}S-labeled wt-N and N mutants with or without the P protein were immunoprecipitated with anti-N or anti-P protein antibodies, respectively. The N protein that was expressed alone showed a phosphorylation pattern different from that of the N protein that bound to the P protein (Fig. 1A and B), suggesting that the N-P protein interaction affects the phosphorylation status of the N protein. To further evaluate these changes, we rescued recombinant viruses whose N protein phosphorylation sites were substituted (rMV-S479A, rMV-S510A, and rMV-S479A/S510A) by reverse genetics and investigated the phosphorylation status of the N protein in cells infected with recombinant viruses at 2 dpi. The N protein in the rMV-infected 293SLAM cells showed the same phosphorylation pattern as the N protein in cotransfected cells (Fig. 1B and C). This implies that the N-phosphorylation of rMVs in the infected cells was also affected by the N-P protein association.

The N protein expressed alone in cultured cells is imported into the nucleus, and the presence of the P protein retains the N protein in the cytoplasm (26). Therefore, we examined whether changes in N-phosphorylation through the N-P interaction depend upon the change in localization or on the binding of the N and P proteins. In our previous report, a nuclear localization signal was identified in the N protein; therefore, we generated an N protein mutant (74–77A, referred to as mN) that localized to the cytoplasm (27). We compared the phosphorylation levels of the wt-N and mN expressed alone or with the P protein. The phosphorylation level of the wt-N protein associated with the P protein was 37.4% of that of the free wt-N protein in HEK293 cells (Fig. 2A). The mN protein expressed with the P protein also had a reduced phosphorylation level (35.6%) compared with the free mN protein (Fig. 2B). This indicates that the N-phosphorylation level was directly downregulated by N-P protein binding and was not affected by the localization of the N protein.

One- and multistep growth kinetics of rMVs. To investigate the influence of N-phosphorylation on virus production, we compared the one- and multistep virus growth kinetics of wt-MV and rMVs (S479A, S510A, and S479A/S510A). Released and cell-associated viruses were harvested at 4 to 24 hpi (one-step growth) and 0.5 to 6 dpi (multistep growth) and their titers determined. In the one-step analysis, rMV-S479A/S510A rapidly replicated and reached the peak titer at 20 hpi, while the wt-MV showed slower growth kinetics until 20 hpi. The titer of wt-MV at 24 hpi was the same as or slightly higher than that of rMV-S479A/S510A. In one-step growth, rMV-S479A and rMV-A510A showed moderate replication levels; however, the peak titer for rMV-S479A was the lowest. The cell-free rMVs showed growth kinetics similar to those of the cell-associated viruses (Fig. 3A and B). Conversely, in multistep growth kinetics, rMV-S479A/S510A propagated most efficiently and showed higher peak titers. These titers remained high during the plateau phase of viral growth (around 3 to 6 dpi). The level of growth of rMV-S479A was lowest, while other viruses showed moderate growth levels (Fig. 3C and D). Although rMV-S479A replicated faster than wt-MV in one-step growth kinetics, it

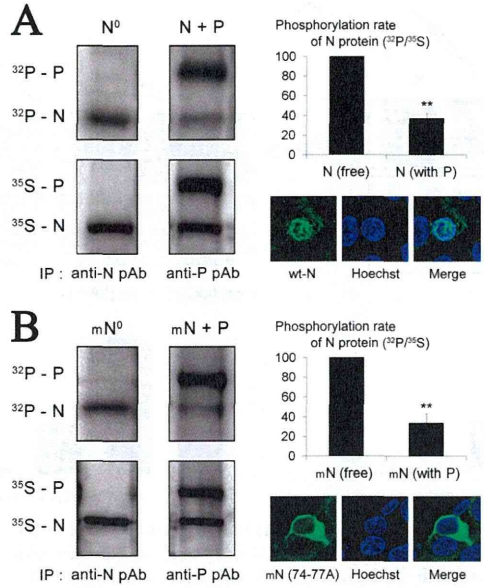

FIG 2 Phosphorylation of free N protein (N^0) and P-associated N protein. (A) HEK293 cells transiently expressing wt-N protein, with or without the P protein, were labeled with ^{32}P or ^{35}S and immunoprecipitated (IP) with anti-N or anti-P antibodies (pAb) as appropriate. The bar graph shows the relative phosphorylation levels (^{32}P-N/^{35}S-N) of the N protein. Error bars indicate standard deviations. **, $P < 0.01$. The location of the wt-N protein was shown by immunofluorescence using the 8G anti-N monoclonal antibody (25), with nuclei stained with Hoechst 33342. (B) The same experiment was conducted using an N protein mutant (mN, 74–77A).

could not maintain a higher titer than the other viruses during the latter phases of multistep growth. The different characteristics in the early and late phases of growth suggested that N-phosphorylation has multiple roles in the virus life cycle.

To investigate the influences of N-phosphorylation on viral growth, we performed a time course analysis of N gene expression. Recombinant virus-infected 293SLAM cells were harvested at each time point and N proteins detected by immunoblotting. Accumulation of the N protein (Fig. 4A and B) was almost similar to the growth rates (Fig. 3) in the one-step and multistep growth analysis, suggesting that the differences in growth kinetics between wt-MV and rMVs were caused by changes in viral gene expression levels. It also suggests that N-phosphorylation is involved in the regulation of viral gene expression. It has been reported that transcription of the MV N protein induces expression of cytokines, such as RANTES, in a dose-dependent manner (28); therefore, we also evaluated whether these changes in viral gene expression affected induction of the host immune response. Induction of cytokines was significantly lower for wt-MV than for rMV-S479A/S510A and rMV-S510A (Fig. 4C and D). Infection with the rMV-S479A mutant also tended to induce higher cytokine levels than wt-MV infections. Therefore, it can be seen that upregulation of viral gene expression during the early phase of rMV infection was accompanied by high levels of cytokine induction.

To further evaluate the influence of N-phosphorylation on virus growth, we investigated the relative phosphorylation levels of the N protein at each time point. From 16 hpi to 6 dpi, the relative phosphorylation level of the N protein was constant in the 293SLAM cells (Fig. 4E). During the multistep growth analysis, viral titers at the plateau phase inversely correlated with the phosphorylation level of the N protein. Titers for the cell-free virus showed a high inverse correlation with N-phosphorylation intensity, with a coefficient of determination (R^2) of 0.82 ($P < 0.001$) at 3 to 6 dpi (Fig. 4F). The R^2 for the cell-associated virus was 0.69 ($P < 0.001$) and was also significantly inversely correlated (Fig. 4G). These regression curves showed exponential trend lines. The intensity of N-phosphorylation seems to have a strong influence on the plateau-phase titer during multistep growth. Intensely phosphorylated N protein caused a reduction in the viral titer during the latter phase of infection. Conversely, N-phosphorylation intensity and early-phase viral titers did not show a significant correlation, suggesting that the difference in virus growth levels during the early phase of infection was not caused by different phosphorylation intensities of the N-protein. Taking the results together, N-phosphorylation status affects virus gene expression and N-phosphorylation intensity affects the titers selectively during the plateau phase of multistep growth kinetics.

Nucleocytoplasmic trafficking and N-M protein interaction are independent of N-phosphorylation. The phosphorylation sites of the N protein are within the C-terminal tail region, and therefore we focused on the influence of N protein C-terminal functions, such as nucleocytoplasmic transport (27) and binding to the P protein (29) and M protein (30). Our previous research identified a nuclear export signal and a nuclear localizing signal for the MV N protein. These signal sequences were prerequisites for nucleocytoplasmic transport (27). The N protein is imported into the nucleus; however, its trafficking mechanism(s) and significance have not been fully clarified. Transiently expressed wt-N and its phosphorylation mutants in HEK293 cells were mainly localized in nuclear foci, with no significant difference in localization observed (Fig. 5A). This suggests that nuclear trafficking of the N protein is not under the regulation of N-phosphorylation.

It is apparent that the N-P protein interaction is not affected by the phosphorylation status of the N protein (Fig. 1B). The M protein also associates with the N protein tail region and assists in virus assembly (30). N protein mutants and the M protein were transiently coexpressed in HEK293 cells, and a coimmunoprecipitation assay was conducted. As a result, no significant changes in N-M association were observed among N protein mutants (Fig. 5B). Moreover, in the presence of the P protein, there was also no difference in the levels of coimmunoprecipitation of the wt-N and the N mutants or the P and M proteins (Fig. 5C). To investigate the influence of other viral proteins on N, P, and M protein binding, we conducted immunoprecipitation experiments using wt-MV- or rMV-infected cells. As with the transcription experiment, no differences were observed in N, P, and M protein interaction (data not shown). Taken together, these results indicate that nuclear trafficking of the N protein, N-P interactions, and N-M interactions are not regulated by N-phosphorylation. Alterations in growth of the rMVs were not caused by changes in these factors.

Influence of N-phosphorylation on viral RNA stability. The viral genome tightly associates with the N protein to form the nucleocapsid and is protected from RNases and siRNAs (8, 11, 12). We evaluated turnover of the viral genomic and antigenomic RNAs by pulse-chase experiments to determine any differences in the encapsidation ability of the N protein. Encapsidated RNAs of rMV-S479A were rapidly degraded, while those of rMV-S479A/